Site-Specific Anchoring of Tetrairon(III) Single Molecule Magnets on Functionalized Si(100) Surfaces

Guglielmo G. Condorelli,*,† Alessandro Motta,† Giovanna Pellegrino,† Andrea Cornia,‡ Lapo Gorini,§ Ignazio L. Fragalà,† Claudio Sangregorio,§ and Lorenzo Sorace§

Department of Chemistry, University of Catania and INSTM UdR Catania, V.le A. Doria 6, 95125 Catania, Italy, Department of Chemistry, University of Modena and Reggio Emilia and INSTM UdR Modena, via G. Campi 183, 41100 Modena, Italy, and Department of Chemistry, University of Florence and INSTM UdR Florence, via della Lastruccia 3, 50019 Sesto Fiorentino, Italy

Received December 13, 2007

The site-specific reaction of tetrairon(III) propeller-like clusters with tripodal ligands derived from 2-hydroxymethyl-propane-1,3-diol was investigated as a route to graft these single molecule magnets (SMMs) on Si(100). A silicon surface prefunctionalized with a long-chain trimethylol derivative was reacted with $[Fe_4(OMe)_6(tmhd)_6]$ (**1**) and $[Fe_4(L)_2(tmhd)_6]$ (**2**), and the reaction course was followed by X-ray photoelectron spectroscopy (XPS), attenuated total reflection−infrared spectroscopy, and atomic force microscopy (Htmhd = 2,2,6,6-tetramethylheptane-3,5-dione, H_3L = 2-(4-chloro-phenyl)-2-hydroxymethyl-propane-1,3-diol). Chlorine-marked complex **2** was specifically designed to monitor the ligand-exchange reaction by XPS. This technique showed that the amount of Fe at the surface closely parallels the surface concentration of tripodal receptors. For low receptor concentrations the Cl/Fe atomic ratio is halved as compared with solid **2**, as expected for intact molecules linked to the surface via one receptor only. For high receptor concentrations, the Cl/Fe ratio drops to zero, as expected for a complete replacement of L^{3-} ligands by surface-bound receptors.

Introduction

Single molecule magnets (SMMs) are molecular clusters displaying magnetic hysteresis of pure molecular origin.[1] In these systems, the dynamics of the magnetic moment is subject to an anisotropy barrier, which determines an exceedingly slow relaxation at low temperature and magnetic bistability. As a result of their unique magnetic behavior, SMMs are investigated as elementary units for high-density data storage applications, quantum computing, and spintronics.[2] The search for new SMMs with improved performances, that is, with higher anisotropy barriers,[3] is then accompanied by attempts to organize these molecules on substrates, in such a way that the magnetic state of individual clusters can be probed.[4] Prospects for application of SMMs in molecular electronics find the most promising architecture in hybrid systems in which functional molecules are organized on inorganic substrates,[5] like technologically relevant Si(100) surface.[6] Approaches have been recently described to organize SMMs of the Mn_{12} family on silicon using local oxidation nanolithography, [7a] stamp-assisted deposition,[7b] or surface prefunctionalization with suitable carboxylate receptors.[8] A strategy to control Mn_{12} orientation on the surface has also been proposed.[9]

Mn_{12} complexes have detained for almost 15 years the highest anisotropy barrier for a SMM; however, they are very prone to reduction and fragmentation,[10] which are known to unfavorably affect magnetic properties. Furthermore, controlling the SMM orientation on prefunctionalized surfaces necessarily requires site-specific reactions, which are

* Corresponding author. Telephone (+39) 095-7385069, fax (+39) 095-580138, E-mail guidocon@unict.it.
† University of Catania.
‡ University of Modena and Reggio Emilia.
§ University of Florence.

(1) (a) Sessoli, R.; Gatteschi, D.; Caneschi, A.; Novak, M. A. *Nature* **1993**, *365*, 141–143. (b) Gatteschi, D.; Sessoli, R.; Villain, J. *Molecular Nanomagnets*; Oxford University Press: Oxford, U.K., 2006.
(2) (a) Leuenberger, M. N.; Loss, D. *Nature* **2001**, *410*, 789–793. (b) Chudnovsky, E. M. *Science* **1996**, *274*, 938–939.
(3) (a) Milios, C. J.; Vinslava, A.; Wood, P. A.; Parsons, S.; Wernsdorfer, W.; Christou, G.; Perlepes, S. P.; Brechin, E. K. *J. Am. Chem. Soc.* **2007**, *129*, 8–9. (b) Milios, C. J.; Vinslava, A.; Wernsdorfer, W.; Moggach, S.; Parsons, S.; Perlepes, S. P.; Christou, G.; Brechin, E. K. *J. Am. Chem. Soc.* **2007**, *129*, 2754–2755.
(4) Cornia, A.; Fabretti, C. A.; Zobbi, L.; Caneschi, A.; Gatteschi, D.; Mannini, M.; Sessoli, R. *Struct. Bonding (Berlin)* **2006**, *122*, 133–161.
(5) (a) Joachim, C.; Gimzewski, J. K.; Aviram, A. *Nature,* **2000**, *408*, 541–548. (b) Filip-Granit, N.; Van der Boom, M. E.; Yerushalmi, R.; Scherz, A.; Cohen, H. *Nano Lett.* **2006**, *6*, 2848–2851. (c) Shukla, A. D.; Das, A.; van der Boom, M. E. *Angew. Chem., Int. Ed.* **2005**, *44*, 3237–3240.
(6) (a) Linford, M. R.; Fenter, P.; Eisenberger, P. M.; Chidsey, C. E. D. *J. Am. Chem. Soc.* **1995**, *117*, 3145–3155. (b) Buriak, J. M. *Chem. Rev.* **2002**, *102*, 1271–1308.
(7) (a) Martínez, R. V.; García, F.; García, R.; Coronado, E.; Forment-Aliaga, A.; Romero, F. M.; Tatay, S. *Adv. Mater.* **2007**, *19*, 291–295. (b) Cavallini, M.; Biscarini, F.; Gomez-Segura, J.; Ruiz, D.; Veciana, J. *Nano Lett.* **2003**, *3*, 1527–1530.
(8) (a) Condorelli, G. G.; Motta, A.; Fragalà, I. L.; Giannazzo, F.; Raineri, V.; Caneschi, A.; Gatteschi, D. *Angew. Chem., Int. Ed.* **2004**, *43*, 4081–4084. (b) Condorelli, G. G.; Motta, A.; Favazza, M.; Nativo, P.; Fragalà, I. L.; Gatteschi, D. *Chem. Eur. J.* **2006**, *12*, 3558–3566.
(9) Fleury, B.; Catala, L.; Huc, V.; David, C.; Zhong, W. Z.; Jegou, P.; Baraton, L.; Palacin, S.; Albouy, P.-A.; Mallah, T. *Chem. Commun.* **2005**, *15*, 2020–2022.
(10) Voss, S.; Fonin, M.; Rüdiger, U.; Burgert, M.; Groth, U.; Dedkov, Y. S. *Phys. Rev. B* **2007**, *75*, 045102.

10.1021/cm703561c CCC: $40.75
Published on Web 02/27/2008

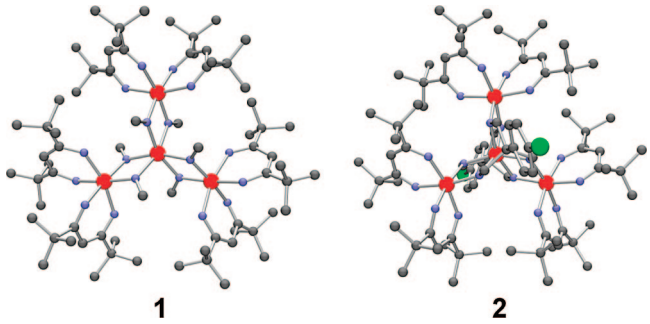

Figure 1. Molecular structure of clusters **1** and **2** viewed approximately along the idealized 3-fold axis. Color code: red = Fe; blue = O; gray = C; green = Cl. H atoms omitted for clarity.

difficult to carry out on the Mn_{12} core.[11] As an alternative, we are currently pursuing the silicon grafting of robust, propeller-like tetrairon(III) clusters derived from $[Fe_4(OMe)_6(tmhd)_6]$ (**1**) (Figure 1), which represents one of the simplest systems showing SMM behavior (Htmhd = 2,2,6,6-tetramethylheptane-3,5-dione).[12] As a major advantage, in complex **1** the bridging and nonbridging ligands can be varied independently from each other. In particular, the six methoxide bridges can be selectively exchanged and replaced by two tripodal ligands derived from 2-hydroxymethyl-propane-1,3-diol, $[R\text{-}C(CH_2OH)_3]$ (Scheme 1), allowing a site-specific functionalization of the cluster core with a variety of R groups.[13] It was previously suggested that the binding properties of the trimethylol function toward the Fe_4 core might be exploited to graft these molecules on solid substrates.[13a]

In this paper we describe the preparation of a Si(100) surface functionalized with tripodal receptors derived from 2,2-bis(hydroxymethyl)-10-undecen-1-ol (H_3Z), which was shown to actively bind the Fe_4 core (Scheme 1).[13c] The surface was then reacted with **1** and $[Fe_4(L)_2(tmhd)_6]$ (**2**), where H_3L = 2-(4-chloro-phenyl)-2-hydroxymethyl-propane-1,3-diol (Scheme 1). The reaction was followed using X-ray photoelectron spectroscopy (XPS), attenuated total reflection (ATR)-IR spectroscopy, and atomic force microscopy (AFM). In particular, the chlorine-marked compound **2** was specifically designed to monitor the ligand-exchange reaction by XPS.

Experimental Section

All chemicals, unless otherwise noted, were commercially available and used as received. Solvents for substrate cleaning were purified by distillation. 1-Octene was distilled over P_2O_5, while mesitylene, diethyl ether, and tetrahydrofuran (THF) were distilled over Na metal. Ethyl acetate and triethylamine were dried over $MgSO_4$ and KOH, respectively, and distilled before use. Complex **1** was prepared as described elsewhere.[13b]

Scheme 1

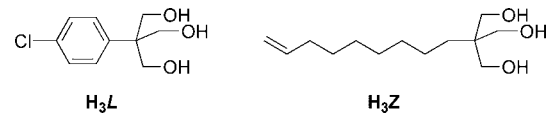

H_3L H_3Z

Acetic Acid 2,2-Bis-acetoxymethyl-undec-10-enyl Ester (Ac_3Z). H_3Z (0.739 g, 3.21 mmol), prepared according to a literature procedure,[14] was dissolved in dry ethylacetate (15 mL). Distilled acetyl chloride (1.134 g, 14.4 mmol) and, subsequently, anhydrous triethylamine (1.461 g, 14.4 mmol) were added dropwise with vigorous stirring. The mixture was stirred overnight and then treated with 20 mL of water and 20 mL of ethyl acetate. The organic layer was separated, washed with water (2 × 25 mL), and dried over $MgSO_4$. Concentration and purification by column chromatography (silica gel, petroleum ether 40–60°/ethyl acetate, 2:1) afforded Ac_3Z as a pale-yellow oil (0.926 g, 81%). ^{1}H NMR (200 MHz, $CDCl_3$): δ (ppm) 4.02 (s, 6H, C(1)H_2); 5.80 (m, 1H, C(10)H), 5.04−4.89 (m, 2H, C(11)H_2); 2.06 (s, 9H, CH_3); 2.02 (m, 2H, C(9)H_2); 1.36−1.27 (m, 12H, C(3-8)H_2).

4-Chlorophenylacetaldehyde. To a solution of 4-chlorophenethyl alcohol (5.0 g, 32 mmol) in dichloromethane (100 mL) at 0 °C was added trichlorocyanuric acid (11 g, 32 mmol). The suspension was stirred for 5 min, and then 2,2,6,6-tetramethylpiperidinyloxy free radical (TEMPO, 70 mg, 0.32 mmol) was added. After 10 min of stirring, the suspension was filtered on celite. The organic mixture was washed with saturated Na_2CO_3 solution (×3), 1 M HCl solution (×3), and brine. The solution was dried on Na_2SO_4 and filtered. The product was obtained as a pale yellow solid (98% yield). ^{1}H NMR (300 MHz, d_6-DMSO): δ (ppm) 9.54 (s, 1H, CHO); 7.21 (m, 2H, Ar); 7.12 (m, 2H, Ar); 3.66 (s, 2H, CH_2).

2-(4-Chloro-phenyl)-2-hydroxymethyl-propane-1,3-diol (H_3L). To a solution of 4-chlorophenyl acetaldehyde (4.8 g, 31 mmol) in dry THF (20 mL) were added paraformaldehyde (6.15 g, 205 mmol) and $Ca(OH)_2$ (18.3 g, 247 mmol). The mixture was stirred into a closed pyrex reaction vial for 4 days at 65 °C. Dichloromethane was added to the mixture, which was then filtered on celite. The solution was dried under vacuum and the solid purified by chromatography (eluent dichloromethane: methanol = 20:1). The product was obtained as a white solid (42% yield). ^{1}H NMR (300 MHz, d_6-DMSO): δ (ppm) 7.47 (m, 2H, Ar), 7.34 (m, 2H, Ar), 4.49 (t, J = 0.73 Hz, 3H, OH), 3.71 (d, J = 0.73 Hz, 6H, CH_2).

$[Fe_4(L)_2(tmhd)_6]\cdot$2EtOH (2·2EtOH). To a solution of **1** (40 mg, 0.027 mmol) in diethyl ether (15 mL) was added a solution of H_3L (13 mg, 0.060 mmol) in diethyl ether/methanol (10:1 v/v), and the mixture was stirred for 10 min at room temperature. Vapor diffusion of dry methanol into the orange solution afforded the product in 24 h (39 mg, 80%). The crystals used for X-ray data collection were obtained by using nondistilled diethyl ether, which explains the presence of the ethanol molecules of crystallization in the structure. Anal. Calcd (%) for $C_{90}H_{146}O_{20}Cl_2Fe_4$: C, 58.67; H, 7.99; Fe, 12.12. Found: C, 59.63; H, 7.90; Fe, 12.41. ^{1}H NMR (303 K, 200 MHz, $CDCl_3$): δ (ppm) 10.5 (s, br, tBu), 11.8 (s, br, Ar), −14 (s, vbr, =CH−).

Single-crystal X-ray data for **2**·2EtOH were collected at 150(2) K on an Oxford Diffraction Xcalibur3 diffractometer equipped with

(11) Pacchioni, M.; Cornia, A.; Fabretti, A. C.; Zobbi, L.; Bonacchi, D.; Caneschi, A.; Chastanet, G.; Gatteschi, D.; Sessoli, R. *Chem. Commun.* **2004**, *260*, 2604–2605.

(12) Barra, A. L.; Caneschi, A.; Cornia, A.; Fabrizi de Biani, F.; Gatteschi, D.; Sangregorio, C.; Sessoli, R.; Sorace, L. *J. Am. Chem. Soc.* **1999**, *121*, 5302–5310.

(13) (a) Cornia, A.; Fabretti, A. C.; Garrisi, P.; Mortalò, C.; Bonacchi, D.; Gatteschi, D.; Sessoli, R.; Sorace, L.; Wernsdorfer, W.; Barra, A.-L. *Angew. Chem., Int. Ed.* **2004**, *43*, 1136–1139. (b) Accorsi, S.; Barra, A. L.; Caneschi, A.; Chastanet, G.; Cornia, A.; Fabretti, A. C.; Gatteschi, D.; Mortalò, C.; Olivieri, E.; Parenti, F.; Rosa, P.; Sessoli, R.; Sorace, L.; Wernsdorfer, W.; Zobbi, L. *J. Am. Chem. Soc.* **2006**, *128*, 4742–4755. (c) Barra, A.-L.; Bianchi, F.; Caneschi, A.; Cornia, A.; Gatteschi, D.; Gorini, L.; Gregoli, L.; Maffini, M.; Parenti, F.; Sessoli, R.; Sorace, L.; Talarico, A. M. *Eur. J. Inorg. Chem.* **2007**, 4145–4152.

(14) Muth, A.; Asam, A.; Huttner, G.; Barth, A.; Zsolnai, L. *Chem. Ber.* **1994**, *127*, 305–311.

Mo Kα radiation. Details on data collection and structure solution and refinement and a full listing of bond distances and angles are available as Supporting Information.

Complex **2** was characterized by magnetic measurements using a Cryogenic S600 SQUID magnetometer. Susceptibility data were recorded on microcrystalline samples with 10 kOe and 1 kOe applied fields in the temperature intervals 50–300 K and 2–50 K, respectively. Isothermal magnetization was measured at 2.2 and 3.7 K in fields up to 6.5 T. High frequency electron paramagnetic resonance (HF-EPR) spectra of a microcrystalline sample of **2** pressed in a pellet were recorded at 190 GHz using a spectrometer hosted at the Grenoble High Magnetic Field Laboratory.

Monolayer Preparation. Mixtures of Ac_3Z (mole fractions $\chi = 1, 0.1, 0.05, 0.02, 0.01, 0$) and 1-octene were dissolved in mesitylene (solution concentration 0.3 M). A 2 mL sample of the alkene solution was placed in a chamber with a quartz window and was deoxygenated by stirring in a dry box for at least 1 h. A Czochralski grown boron doped Si(100) substrate was treated in a piranha solution for 12 min, rinsed in water for 2 min, etched in 1.0% hydrofluoric acid for 90 s, quickly rinsed in water, dried with N_2, and immediately placed in the alkene solution. The chamber remained under UV irradiation (254 nm) for 2 h. The sample was then removed from the solution and sonicated in dichloromethane for 5 min.

Removal of protecting groups was performed according to a method reported by Strother et al.[15] Briefly, the grafted surfaces were dipped in a solution of potassium *tert*-butoxide in DMSO (250 mM) for 80 s at room temperature followed by rinsing in acidified water (100 nM HCl).

The prefunctionalized silicon substrate was dipped in a solution of **1** or **2** in anhydrous diethyl ether (3×10^{-5} M) in a glovebox at room temperature for 1 h or 6 h, respectively. The substrate was removed from the solution and sonicated in diethyl ether and dichloromethane for 5 min to remove unreacted Fe_4 molecular clusters.

The XPS spectra were recorded with a PHI ESCA/SAM 5600 Multy technique spectrometer equipped with a monochromatized Al Kα X-ray source. Unless otherwise noted, the analyses were carried out either at 45° or at 20° photoelectron take-off angle relative to the sample surface with an acceptance angle of ±7°. The binding energy (BE) scale was calibrated by centering the adventitious/hydrocarbon carbon C 1s at 285.0 eV.[16]

ATR-IR spectra of the monolayers were recorded on JASCO FTIR 430 equipped with a Harrick GATR germanium single reflection accessory, collecting the spectra with 80 scans at 4 cm^{-1} resolution.

AFM images were obtained in high amplitude mode (tapping mode) by a NT-MDT instrument. The noise level before and after each measurement was 0.01 nm.

Results and Discussion

Synthesis, Structure, and Magnetic Properties of 2. The new, chlorine-marked complex **2** was obtained by reacting **1** with an excess of H_3L and by crystallization from Et_2O/MeOH mixtures. The compound was characterized by a single-crystal X-ray diffraction investigation, which confirmed the expected molecular structure (Figure 1). The magnetic behavior of **2**, shown in Figure 2 as a $\chi_m T$ versus T plot, is characteristic of SMMs of the Fe_4 family, in which dominant antiferromagnetic interactions stabilize an $S = 5$ ground spin state (χ_m is the molar magnetic susceptibility).[13] Quantitative fitting of $\chi_m T$ data at $T > 20$ K using a Heisenberg plus Zeeman spin Hamiltonian afforded $g = 1.976(4)$, $J_1 = 16.0(1)$ cm^{-1}, and $J_2 = 0.0(1)$ cm^{-1}, where J_1 and J_2 are the nearest-neighbor and next-nearest neighbor exchange-coupling constants, respectively.[13] The isothermal molar magnetization recorded at 2.2 and 3.7 K (inset in Figure 2) approaches 10 $N_A\mu_B$ in the high field limit, thus confirming the presence of an $S = 5$ ground state.

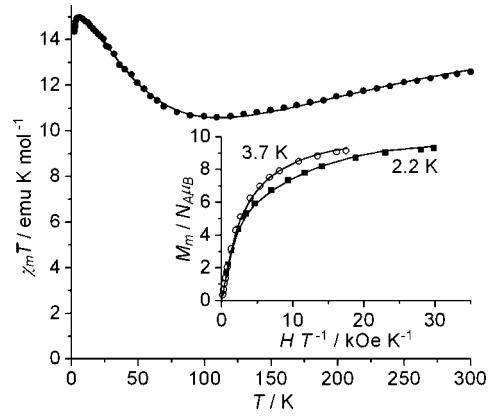

Figure 2. $\chi_m T$ vs T plot for a powder sample of **2.** The inset shows the field dependence of the isothermal magnetization at 2.2 and 3.7 K. Solid lines provide the best fit to experimental data with the parameters reported in the text.

The noncoincidence of isothermal magnetization curves when plotted against H/T is a signature of magnetic anisotropy, which was evaluated by fitting magnetization data with an axial zero-field splitting plus Zeeman Hamiltonian[13] to give $D = -0.42(2)$ cm^{-1} and $g = 1.96(1)$. The occurrence of a zero-field split $S = 5$ ground state is also demonstrated by HF-EPR spectra at 190 GHz (Figure 3). The characteristic patterns of parallel and perpendicular transitions are clearly observed in low fields and high fields, respectively. In addition, all resonances are partially structured, suggesting the presence of two magnetically inequivalent species in the sample, with relative abundance 6:1. Quantitative simulation of HF-EPR spectra[17] was accomplished using the spin Hamiltonian

$$\hat{H}_{EPR} = \mu_B \hat{\mathbf{S}}\cdot\mathbf{g}\cdot\hat{\mathbf{H}} + D\hat{\mathbf{S}}_z^2 + B_4^0\hat{\mathbf{O}}_4^0 + \frac{1}{2}E(\hat{\mathbf{S}}_+^2 + \hat{\mathbf{S}}_-^2) \qquad (1)$$

which is consistent with the 2-fold molecular symmetry observed in X-ray studies and afforded the following best-fit parameters: (for the majority species) $D = -0.411$ cm^{-1}, $B_4^0 = 1.1 \times 10^{-5}$ cm^{-1}, $E = 0.010$ cm^{-1}; (for the minority species) $D = -0.400$ cm^{-1}, $B_4^0 = 1.0 \times 10^{-5}$ cm^{-1}, $E = 0.010$ cm^{-1} with $1.992 < g < 1.995$. The two species presumably reflect the slightly different environments generated by the partial loss of crystallization solvent. Inspection of the D values found in the other doubly substituted Fe_4 complexes so far magnetically and structurally characterized (R = Me,[13a,b] $(CH_2)_7CH{=}CH_2$,[13c] Ph[13b]) reveals that **2** is the least anisotropic derivative. This datum confirms the crucial role played by the propeller's pitch γ in determining magnetic anisotropy,[13b] because the present complex has the smallest pitch in the series (67.3°).

(15) Strother, T.; Cai, W.; Zhao, X.; Hamers, R. J.; Smith, L. M. *J. Am. Chem. Soc.* **2000**, *122*, 1205–1209.
(16) Swift, P. *Surf. Interface Anal.* **1982**, *4*, 47–51.
(17) Mossin, S.; Weihe, H.; Barra, A.-L. *J. Am. Chem. Soc.* **2002**, *124*, 8764–8765.

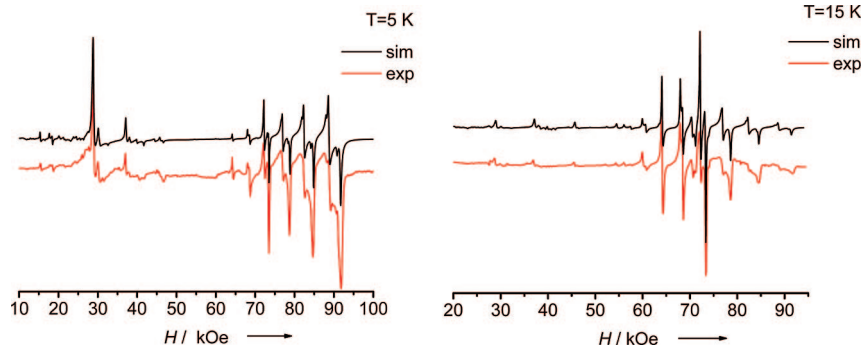

Figure 3. HF-EPR (190 GHz) spectra recorded on a pressed pellet of **2** at two different temperatures, 5 K (on the left) and 15 K (on the right).

Scheme 2. Three Step Process Adopted for SMM Anchoring on Si(100)

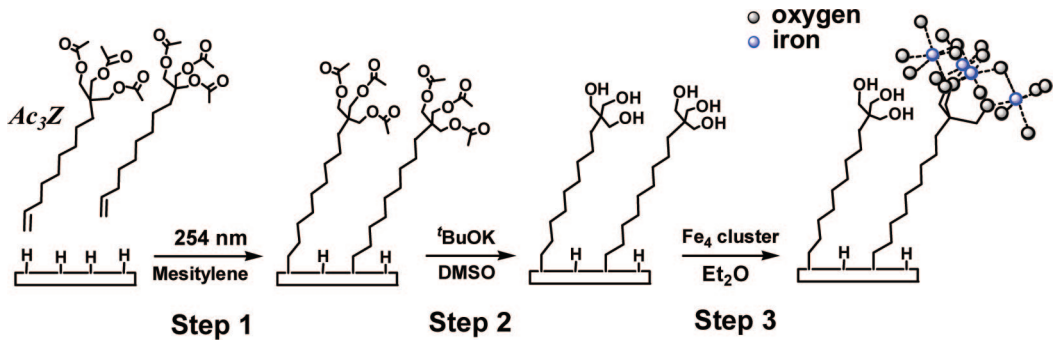

Monolayer Preparation. The devised anchoring strategy encompasses three steps (Scheme 2): (1) grafting of acetyl-protected H_3Z (Ac_3Z), in pure form or mixed with 1-octene, on hydrogen-terminated silicon by photoinduced hydrosilylation; (2) alkaline hydrolysis to liberate the hydroxylic functions, and (3) ligand exchange on **1** and **2**. Notice that the feasibility of the triol exchange reaction

$$[Fe_4(L)_2(tmhd)_6] + nH_3Z \rightleftarrows [Fe_4(L)_{2-n}(Z)_n(tmhd)_6] + nH_3L \quad (n = 1, 2) \quad (2)$$

was proven by proton NMR spectroscopy in solution (see Supporting Information).

Each reaction step was monitored by XPS, which provided evidence for all the expected elements in the grafted layers (see also Supporting Information).

The C 1s signal observed after hydrosilylation is a reliable indicator of the successful grafting of Ac_3Z.

As compared with freshly etched silicon (Figure 4a), the C 1s peak shows an enhanced intensity and a richer structure (Figure 4b). It consists of three main components centered at 285.0 eV (C^0, aliphatic hydrocarbons), 287.0 eV (C^{+1}, $-O-CH_2-$ groups of esters), and 289.5 eV (C^{+3}, ester carbonyl groups).[18] To fit experimental spectra, two additional components at 286.0 and 283.5 eV have to be added. The former component can be due either to the methyl groups secondarily shifted by the presence of adjacent $-C(O)O-$ moieties[18b] or to slightly oxidized carbon contaminants generated by chemical manipulations.[19] The latter band is ascribed to the Si−C bond that forms upon hydrosilylation reaction.[8] This component is, however, somewhat hidden because of two factors: (i) the carbon atom involved in the Si−C bond is buried under the grafted monolayer, and the photoemission signal is therefore attenuated; (ii) the presence of proximal SiO_x and SiOH terminations shifts the C^{-1} component to slightly higher BE values, and, hence, the component overlaps with the more intense C^0 band.[19]

After the hydrolysis the total intensity of the C 1s signal decreases considerably (Figure 4c). The band associated to the carbonyl groups (289.5 eV) is substantially depressed, even though it is still detectable, indicating the presence of residual ester functionalities. The reaction with either **1** or **2** leads to an overall increase of the C 1s signal (Figure 4d), whose broad component at 286–287 eV is consistent with

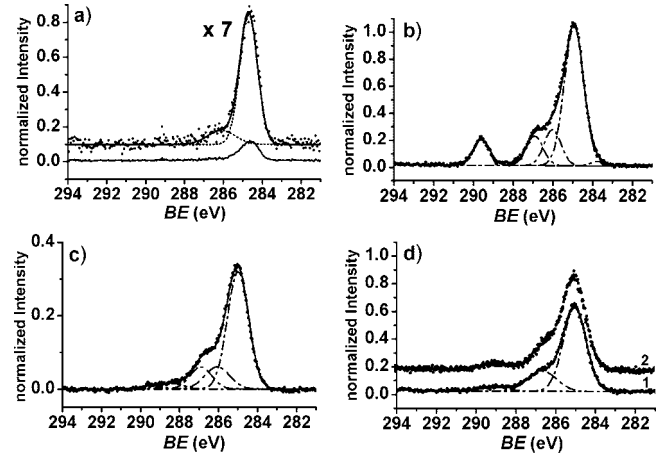

Figure 4. High resolution C 1s XPS band of freshly etched silicon surface (a) and of samples obtained after the reaction with Ac_3Z (b), followed by hydrolysis (c) and anchoring of **1** and **2** (d). The intensities are normalized to the total Si 2p intensity. For clarity, the spectrum of **2** is reported with a 0.2 *y*-axis shift. Take-off photoelectron angle was 45° relative to the surface.

(18) (a) Gulino, A.; Lupo, F.; Condorelli, G. G.; Mineo, P.; Fragalà, I. L. *Chem. Mater.* **2007**, *19*, 5102–5109. (b) Briggs, D.; Beamson, G. *Anal. Chem.* **1992**, *64*, 1729–1736.

(19) Condorelli, G. G.; Motta, A.; Favazza, M.; Fragalà, I. L.; Busi, M.; Menozzi, E.; Dalcanale, E.; Cristofolini, L. *Langmuir* **2006**, *22*, 11126–11133.

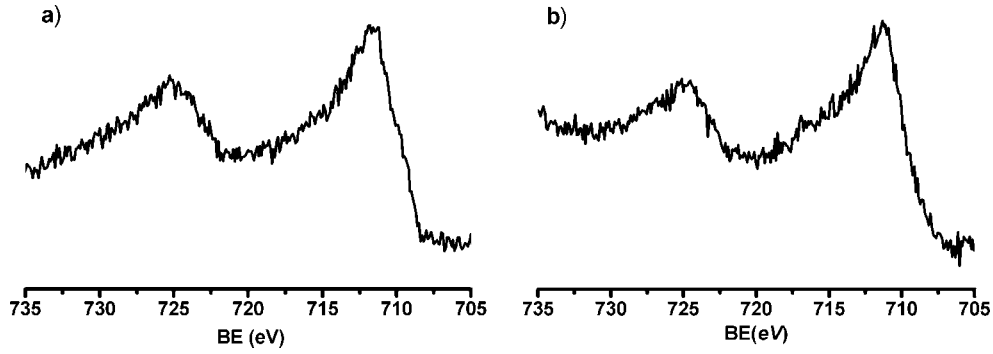

Figure 5. High resolution XPS Fe 2p bands of (a) the molecular cluster **2** anchored on prefunctionalized silicon with pure tripodal ligand and (b) a microcrystalline sample of cluster **2**.

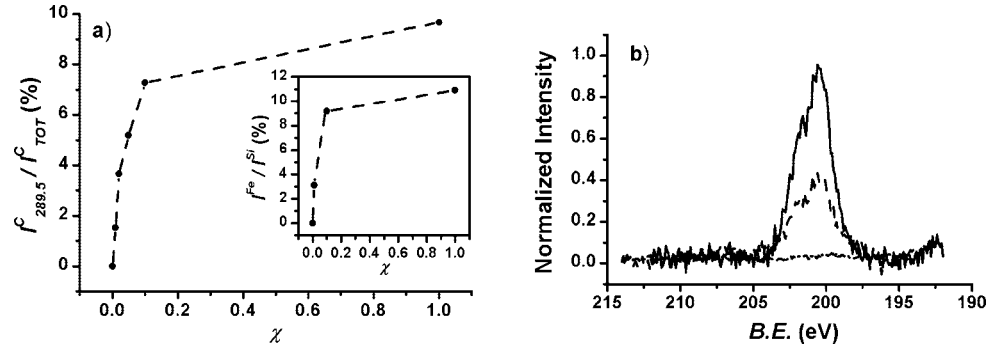

Figure 6. (a) Grafted layer composition vs the molar fraction of Ac_3Z (χ) used in the hydrosilylation reaction. (b) High resolution XPS bands of Cl 2p region for different χ values obtained after the reaction with **2**. Straight line, microcrystalline powders; dashed line, $\chi = 0.01$; dotted line, $\chi = 1$. Take-off photoelectron angle was 20° relative to the surface.

Scheme 3. Possible Geometric Arrangements for the Molecular Cluster Anchoring on the Functionalized Surface

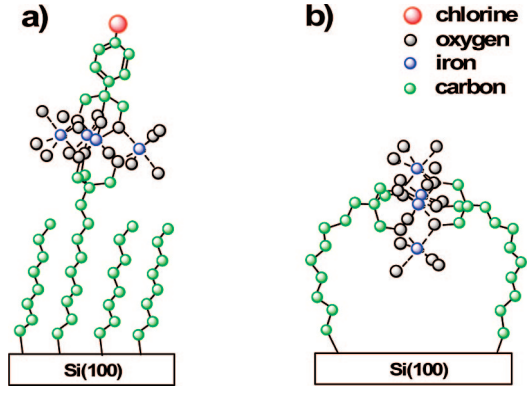

the presence of the alkoxide and β-diketonate groups of Fe_4 molecular clusters.

The anchoring of **1** and **2** is however most directly supported by the presence of a doublet in the Fe 2p region (BE Fe $2p_{3/2}$ = 711.0 eV in Figure 5a).

The position and the shape of Fe band are similar to those detected on microcrystalline samples of **1** and **2** (Figure 5b) and are in good agreement with the presence of Fe^{+3} species.[20]

To check the expected correlation between the amount of Fe and the concentration of tripodal receptors, the silicon surface was functionalized with various mixtures of 1-octene and Ac_3Z. The surface density of the latter was monitored by the fraction of carbonyl-type C 1s signal ($I_{289.5}{}^{C}/I_{Tot}{}^{C}$).

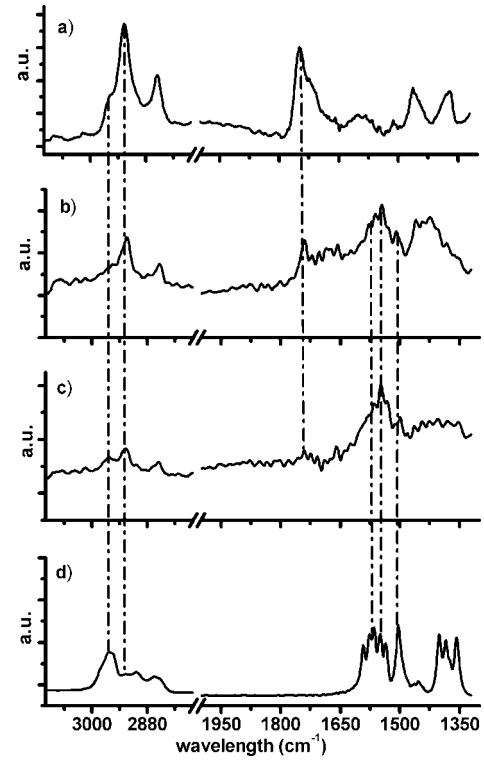

Figure 7. ATR-IR spectra of (a) pure Ac_3Z grafted on silicon; (b, c) complex **2** anchored on the functionalized surface after ligand deprotection performed with (b) 30 s and (c) 80 s hydrolysis; and (d) a microcrystalline sample of **2**.

As shown in Figure 6a, the latter increases with the molar fraction (χ) of Ac_3Z in the mixture used for the hydrosilylation reaction. Noticeably, the I^{Fe}/I^{Si} intensity ratio observed

(20) Blomquist, J.; Helgeson, U.; Moberg, L. C.; Folkesson, B.; Larsson, R. *Inorg. Chim. Acta* **1983**, *69*, 17–23.

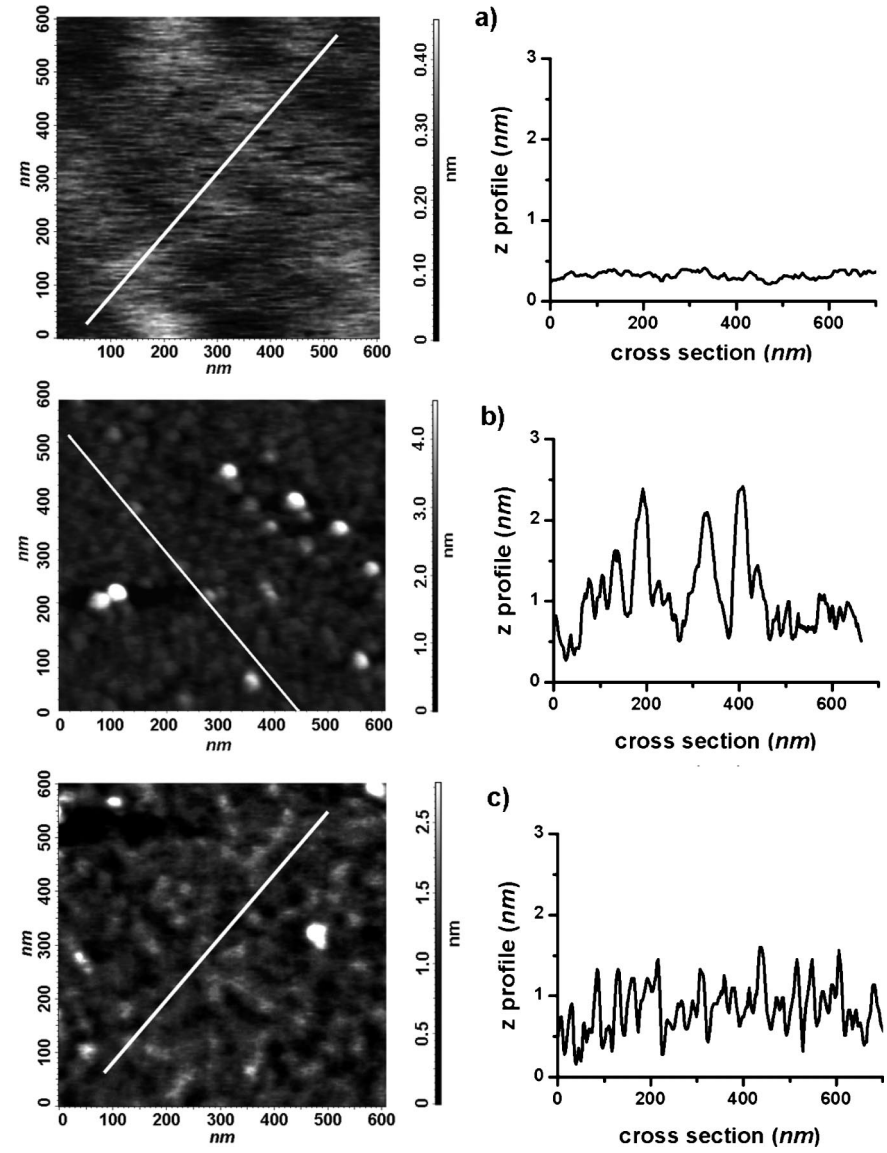

Figure 8. AFM images and cross sections of (a) Ac_3Z grafted on silicon; (b) complex **2** anchored on pure Ac_3Z ($\chi = 1.0$); and (c) complex **2** anchored on Ac_3Z/1-octene mixtures ($\chi = 0.01$).

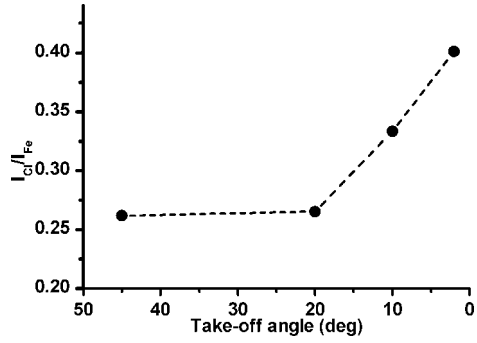

Figure 9. Dependence of the Cl/Fe signal ratio upon the take-off angle with respect to the surface plane.

after reaction with **2** (Figure 6a, inset) follows the same trend. We remark that in the absence of tripodal receptors no significant signal is detected in the Fe region.

The presence of two chlorine atoms per molecule in **2** allowed additional insight to be gained on surface-bound species by monitoring the Cl/Fe ratio. Figure 6b shows the Cl 2p XPS spectra of a microcrystalline sample of **2** and of samples obtained with $\chi = 0.01$ and $\chi = 1$. For $\chi = 0.01$ the normalized Cl intensity (Cl/Fe ratio) is halved as compared with solid **2**, strongly suggesting that for low receptor concentrations the molecular clusters are intact and linked to the surface through one receptor only (Scheme 3a). By contrast, layers of pure tripodal ligand ($\chi = 1$) show a negligible amount of chlorine after the grafting process. This is expected if both L^{3-} ligands are exchanged, which is possible only for high receptor concentrations (Scheme 3b).

The relationship between the surface receptor density and the number of residual L^{3-} ligands was further confirmed by additional experiments in which dense monolayers of Ac_3Z ($\chi = 1$) were subject to only partial hydrolysis by reducing the hydrolysis time to 30 s (see the following ATR-FTIR results). These samples showed a Cl/Fe ratio similar to that detected at low receptor concentrations ($\chi = 0.01$).

ATR-IR spectra were also used to follow both surface prefunctionalization and the reaction with **2**. After the

grafting of pure Ac_3Z (Figure 7a), two spectral regions become diagnostic, namely, that of CH stretching between 3100 and 2700 cm^{-1} and that of C═O stretching around 1740 cm^{-1}.

After 30 s of hydrolysis and reaction with **2**, the C═O signal of protecting acetyl groups is still detectable, even though its intensity is considerably reduced (Figure 7b), indicating the presence of a significant amount of residual ester functionalities. New bands appear around 1550–1600 cm^{-1}, which compare well with those observed in microcrystalline **2** (Figure 7d), and are attributed to the β-diketonate ligands.[21] After 80 s of hydrolysis (Figure 7c), the C═O signal becomes negligible while the β-diketonate bands gain intensity. Moreover, the asymmetric in-plane CH stretching of methyl groups at 2960 cm^{-1} becomes clearly detectable. The greater intensity of tmhd-related IR signals observed for higher concentration of tripodal receptors, combined with XPS results, lends considerable support to the presence of intact Fe_4 SMMs bound to the surface as depicted in Scheme 3.

The morphology of the grafted layers was evaluated by AFM. After the grafting of Ac_3Z (Figure 8a), in pure form or mixed with 1-octene, the surface appears very flat (root mean square, rms = 0.04 nm) with an average vertical size (R_{mean} = 0.25 nm) comparable to that of a freshly etched Si(100) surface.

Samples obtained after reaction of **2** on pure receptor layer (χ = 1.0) show (Figure 8b) dense SMM aggregates with a lateral size of about 30 nm and a structured surface (rms = 0.4 nm) with an R_{mean} value of 1.4 nm comparable with SMM complex diameter (about 1.5 nm).

Samples obtained after anchoring of **2** on a mixed monolayer containing a low receptor concentration (χ = 0.01) show a less structured surface (rms = 0.19 nm) and an average vertical size (R_{mean} = 0.8 nm) of the observed features consistent with the expected height of **2** (Figure 8c). In addition, no evidence of aggregate formation emerges from the AFM images. This behavior is presumably due to the low surface density of the anchoring sites which results in a lower SMM surface concentration (see Figure 6a).

Angle resolved XPS measurements have been also performed on samples obtained after anchoring of **2** on diluted receptor layers to provide further information on the orientation of the anchored molecules.

(21) Nakamoto, K. *Infrared and Raman Spectra of Inorganic and Coordination Compounds*; John Wiley and Sons Inc.: New York, 1978; p 249.

Figure 9 shows the dependence of the Cl/Fe signal ratio upon the take-off angles with respect to the surface plane (45°, 20°, 10°, and 2°). The Cl/Fe signal ratio increases at low take-off angles, thus indicating that the Cl atoms are located above the SMM iron atoms. This behavior is, therefore, in accordance with the presence of an oriented monolayer of Fe_4 SMMs in which the axial ligands bearing the Cl atoms are arranged vertically with respect to the surface. Note, moreover, that the angular dependence of the Cl/Fe ratio cannot be easily reconciled with the formation of a disordered assembly of clusters, thus further indicating that the formation of 3D aggregates of SMMs is precluded on diluted receptor layers.

Conclusion

Fe_4-type SMMs have been reacted with a silicon surface prefunctionalized with site-specific tripodal receptors. A new, chlorine-marked complex **2** was specifically designed to monitor the ligand-exchange reaction by XPS. The surface density of the receptors was shown to control both the amount of Fe, which increases with increasing receptor concentration, and the Cl/Fe ratio at the surface. At low receptor concentrations the Cl/Fe atomic ratio drops to 50% of the value observed in solid **2**, as expected for SMM linked to the surface via one receptor only. For high concentrations of tripodal ligands the Cl/Fe atomic ratio vanishes, suggesting that grafting may occur through two surface-bound tripods.

In addition, angle resolved XPS measurements and AFM showed that the surface density of tripodal ligands is a key point not only for controlling SMM orientation but also for overcoming aggregate formation.

The proposed strategy can be regarded as a viable route to control the surface density and the orientation of SMMs on technological surfaces, which is an important point for the integration of molecules with anisotropic properties on hybrid devices.

Acknowledgment. This work was supported by MIUR through PRIN 2005 (No. 2005031228) and FIRB 2003 (No. RBNE033KMA) projects and by EU through NoE MAGMANet (3-NMP 515767-2). We acknowledge Dr. A.L. Barra (CNRS-Grenoble) for assistance in recording HF-EPR spectra.

Supporting Information Available: Details on data collection, structure solution and refinement, full listing of bond distances and angles (PDF), and CIF file for **2**. High resolution XPS spectra of Si 2p and O 1s regions. Results of proton NMR studies on the triol exchange reaction in solution.

CM703561C